SCANNING TUNNELING MICROSCOPY WITH CHEMICALLY MODIFIED TIPS

Takashi Ito[1] and Yoshio Umezawa[2,*]

[1]*Department of Chemistry, Science University of Tokyo, Shinjuku-Ku, Tokyo 162-8601, Japan*

[2]*Department of Chemistry, School of Science, The University of Tokyo, Bunkyo-Ku, Tokyo 113, Japan*

SUMMARY

As a new approach to chemically selective STM, we have recently revealed and suggested therefrom that tailored chemical modification of STM tips may become a general method for the discrimination of chemical species and functional groups in STM images. STM imagings with gold tips modified with self-assembled monolayers (SAMs) of various organic mercaptans with hydrogen bond donor and acceptor groups permitted selective enhancement of electron tunneling, and as a result enhanced the contrasts of hydroxyl and carboxyl groups as well as ether oxygens in STM images of monolayers formed on graphite. Very similar contrast enhancements for these functional groups can also be obtained with functionalized polymer-modified STM tips. In addition, this method was found to discriminate even two kinds of ether oxygens with different orientations in the monolayers of diethers, $CH_3(CH_2)_{15}O(CH_2)_nO(CH_2)_{15}CH_3$, n=9-12, where the direction of two oxygen lone-pairs could respectively be discriminated with gold tips modified with 4-mercaptobenzoic acid. Not only through hydrogen-bond, coordination-bond-facilitated tunneling was also observed with 4-mercaptopyridine modified gold tips to discriminate metalloporphyrins with different metal centers.

* Corresponding author: phone +81-3-5841-4351; fax +81-3-5841-8349; e-mail umezawa@chem.s.u-tokyo.ac.jp

LIST OF CONTENTS

1 INTRODUCTION

Selective separation and detection in many analytical techniques have been accomplished on the basis of molecular recognition involving various noncovalent interactions such as hydrogen bonds, hydrophobic interactions, and electrostatic interactions at surface and interface. "Tailored" chemical modification of the surface has been often performed for the selective recognition. For example, deliberately attaching appropriate chemical groups to electrode surfaces results in desirable properties such as reagent-based control of the rates and selectivities of electrochemical reactions (chemically modified electrodes) /1/. Also in chromatography, covalent attachment of functional groups to a support allows selective separation of target species /2-4/.

Selective recognition of chemical species on chemically modified surface is also possible in scanning probe microscopies (SPMs), which can probe microscopic and nanoscopic surface structures by scanning with very sharp tips at very close separation from surfaces /5-7/. Among SPMs, scanning tunneling microscopy (STM) and atomic force microscopy (AFM) have recently been used in many laboratories. STM, in which a scanning tip

detects a tunneling current flowing between the conducting tip and surface, can be used for measurements of surface features and the surface electronic structure, and AFM, in which a scanning tip detects a force between tip and sample surface, can be used to measure surface topography. Since 1992, it has been shown that AFM tips modified with self-assembled monolayers (SAMs) or polymers allow the discrimination of surface functional groups on the basis of hydrophobic, electrostatic, and hydrogen bond interactions (chemical force microscopy) /8,9/. In contrast, chemical modification of STM tips for discrimination of surface chemical species was performed by us in 1998 for the first time /10/. Just as in electrochemistry, electron transfer through the overlap of electronic wave functions of tip and sample surfaces plays a central role in STM, which relies on the tunneling effect as operating principle (Figure 1a). This similarity and the success of chemically modified electrodes suggested to us that "tailored" chemical modification of STM tips should allow the control of electron tunneling through rational use of chemical interactions /10/. Here, we mainly review our studies with chemically modified STM tips that allow to discriminate surface chemical species by what seems to be facilitated electron tunneling through hydrogen bond /10-12/ and metal-coordination interactions (Figure 1b) /13/.

2. INFLUENCES OF ADSORBATES ONTO TIPS ON STM IMAGES

Even before we found that chemical modification of STM tips gives selective contrast change in STM images on the basis of hydrogen bond interactions between tip and sample /10/, it had been observed that adsorption of atoms or molecules on a STM tip changes the tip structure /14-16/ and/or electronic states of the tip /14, 16-28/, and causes unexpected changes in the resulting STM images. In this section, we briefly review these reports involving molecular or atomic adsorbates on STM tips.

Halas *et al.* reported that the geometric and electronic structure of STM tips can be controlled by the modification with fullerene (C_{60}). Their first report shows that the adsorption of C_{60} onto STM tips gave the reduction of noise and the enhanced corrugation in the images of graphite surfaces /14/. In addition, they reported that the adsorption of C_{60} on the tip not only resulted in "inverse imaging", which represents a convolution of sample and tip structure /15,16/, but also allowed to image threefold symmetric electron scattering from point defects on a graphite surface even at room temperature

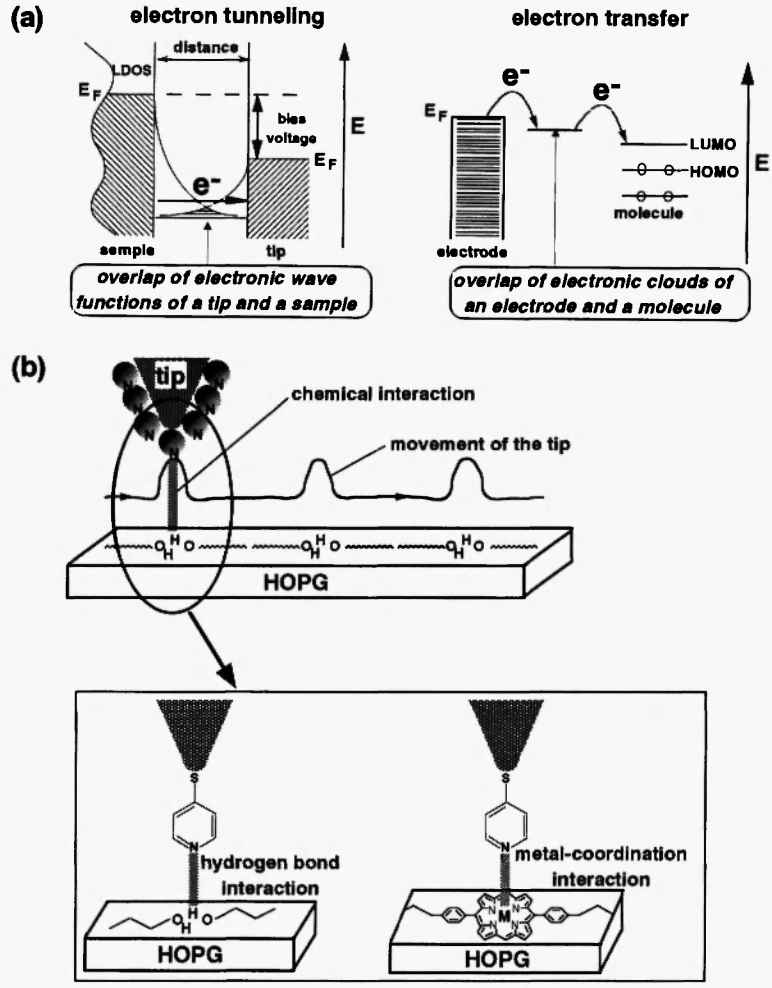

Fig. 1: (a) Comparison of the energy diagrams for electron tunneling in STM (left) and for electron transfer at electrode surface in electrochemistry (right). In the left figure, positive sample bias is applied, and electron tunnel from the tip to the sample. (LDOS : local density of states). In the right figure, negative potential is applied to the electrode, and electrons flow from the electrode to the LUMO of the molecule. (b) Schematic illustration of STM measurements involving electron tunneling facilitated by hydrogen bond (lower left) and by metal-coordination (lower right) interactions between tip-modifying molecule and sample molecule. The line with arrows in the upper figure indicates the *z*-displacement of the tip in a constant current scan over the surface.

/16-18/, which was recently observed with tungsten tips at 77 K /29/. Smalley *et al.* reported that attachment of carbon nanotubes rather than C_{60} to the ends of STM tips allowed to image charge density waves on freshly cleaved TaS_2 surfaces /19/. These results indicate that adsorption of C_{60} and carbon nanotubes to the tip apex alters the geometric structure of the tip and the density of states near the Fermi level of the tip.

It was reported that atomic or molecular adsorbates such as S, O or CO also induced change in STM images, which have been explained on the basis of change in the electronic structure at the tip apex and/or interaction between tip and sample. Contrast changes in STM images of S/Re(0001) /20/ and S/Pt(111) surfaces /21/ were observed when S atoms were adsorbed on the topmost of a tip. These were theoretically explained on the basis of the difference of the external orbitals between the metal atoms and S atom on the tips /20,30,31/. A similar contrast change was reported for the STM images of S/Cu(1111) by the adsorption of S atom onto a tip /27/. Upon the adsorption of a CO molecule on the tip apex, the shapes of NO molecules on Rh(111) in STM images changed from bright ball-like features to ring-shaped features, and this was explained on the basis of p_x and p_y states induced by the CO molecules /23/.

In addition, there are several examples that STM tips having atomic or molecular adsorbates at their apex allowed selective imaging of surface species. Schmid *et al.* reported that Pt and Ni atoms on a $Pt_{25}Ni_{75}(111)$ single crystal surface can be discriminated with tips on which presumably O or S atom had adsorbed /24,25/. Ruan *et al.* showed that metal atoms in ordered overlayers of O on Cu{110} and Ni{110} could be observed with W STM tips with O atoms on the tips, while with bare W tips, only oxygen atoms could be seen /26/. Tips having CO molecules at their apex allowed not only to distinguish CO molecules from oxygen atoms on Cu(111) /28/, but also to give structural information of CO adlayer on Cu(111) surface /22/. These selective imagings were often explained on the basis of some interaction between adsorbed molecules and surface species, although it is unclear what types of interactions induce the selective imagings.

3. CHEMICAL MODIFICATION OF STM TIPS

In many studies described in the above, the atoms or molecules were adsorbed on the tip apex either by their accidental adsorption from the gas

phase onto tip apex /23-26/ or by picking up them from surface onto tip apex /14-18,21,22,28/ under ultrahigh vacuum. In contrast, we prepared STM tips deliberately modified with organic thin films such as SAMs of thiols or conducting polymers in the procedures conventionally used to prepare chemically modified electrodes /1,4/. Except our studies, there is only one report in which STM tips covered with organic thin films were used /32/. STM tips covered with polyaniline containing Cu or Tl_2O_3 clusters were used to investigate the continuity of the polymer film and the presence of metal/insulator/metal (semiconductor) junctions at the end of the prepared tip through electrochemical and STS measurements, but were not used for topographic imaging with the tip. As a result, our study was the first one that showed the selective contrast changes in STM images of surface species observed with chemically modified tips as well as the applicability of such tips to topographic imaging. In this section, we summarize the tip-modification procedures performed in our studies and then the applicability of the tips to STM imaging, before we mention the change in the STM images induced by chemical modification of the tips.

3.1. Tip-Modification Procedures

Chemically modified STM tips can easily be prepared from gold wire by electrochemical etching and subsequent modification procedures. Gold wire was etched in 3 M NaCl at ac 10 V, and then the tips were cleaned in "piranha solution" (7:3 concentrated H_2SO_4:30% H_2O_2; *caution: piranha solution reacts violently with organic compounds and should not be stored in closed containers*). This cleaning procedure seems to allow the removal of organic contaminants on the tip, which sometimes gave images as characteristically observed with chemically modified tips /10/. For SAM modification, the cleaned tips were immersed into 1–10 mM ethanolic solutions of the thiol (**1**–**7**; Figure 2), rinsed with ethanol, and then dried in a stream of nitrogen. On the other hand, polypyrrole films were directly deposited onto gold tips by electrochemical polymerization of pyrroles, which was conducted by dipping tips in aqueous or acetonitrile solutions containing electrolyte and pyrroles. After electrochemical polymerization, tips were washed in an aqueous solution, and dried overnight under ambient conditions. The aqueous solution used to wash the tips modified with polypyrrole is significant, because the observation probability of contrast change due to the tip modification depended strongly on how polypyrrole-

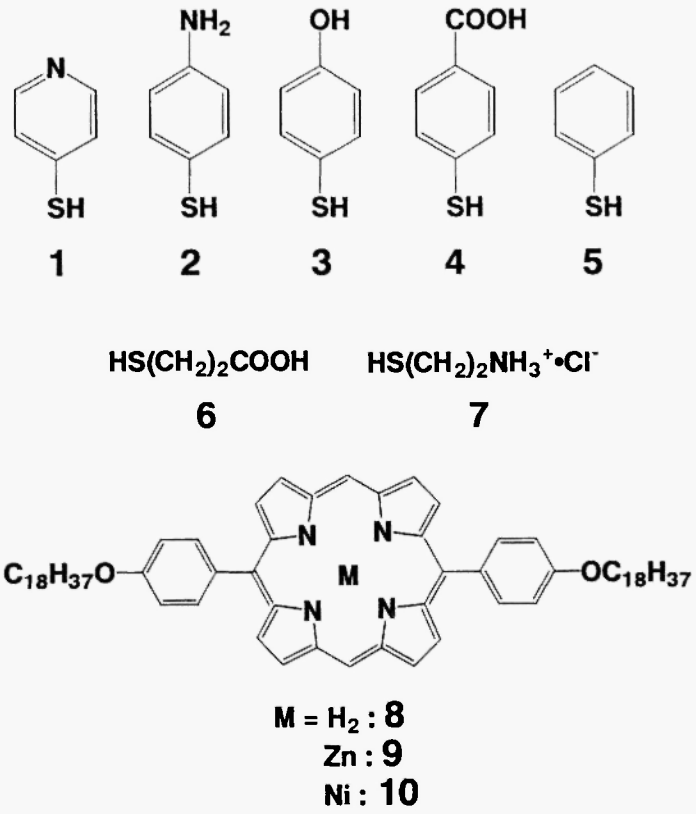

Fig. 2: Chemical structures of thiols **1–7** used for tip modification and porphyrins **8–10** used as samples.

modified tips were washed after the electrochemical polymerization (see **4.2**) /11/.

3.2. STM Imaging with Chemically Modified Tips

Organic molecules, in particular thick polypyrrole films, adsorbing onto STM tips seemed to interfere with STM imaging at high resolution because not only of their lower conductivity but also of the enlargement of tip radius. These problems seemed to be less significant for thiol SAMs because the SAMs were thin enough to allow the electron tunneling and not to change the tip radius. Indeed, the percentage of tips that gave molecular images of 1-octadecanol even for tips modified with SAMs of aromatic thiols **1–5** (77 – 100%) was similar to that for unmodified gold tips (ca. 90%) whereas the

percentage was somewhat lower (51 – 88%) for tips modified with SAMs of aliphatic thiols **6** or **7**. The enhancement of electron transfer through electronic coupling involving aromatic spacers may explain the above difference between aromatic and aliphatic thiols.

For polypyrrole-modified tips, the conductivity of the films strongly affected STM imaging /11/. The tips modified with a highly conductive polypyrrole (BF_4^--doped polypyrrole) gave only a slightly smaller probability (ca. 60%) for the observation of molecular images for 1-octadecanol and 1-octadecanoic acid monolayers than unmodified tips (ca. 90%). In addition, tips modified with BF_4^--doped polypyrrole gave molecular images with high resolution (e.g., Figure 6a), indicating that the polymer films on the tips are fairly hard and that their surface does not change their shapes during scanning /33/. Interestingly, regardless of the thickness of the BF_4^--doped polypyrrole films, the probabilities for observation of molecular images were ca. 60% for 1-octadecanol and 1-octadecanoic acid monolayers, indicating that a sharp tip apex is very important for the observation of molecular images but that the film thickness does not affect the images appreciably /11/. In contrast, tips modified with Cl^--doped polypyrrole gave only low probabilities (ca. 20%) for the observation of molecular images, and, in addition, did not allow observation of the high-resolution images, probably due to the low conductivity of the polymer. These results indicate that tips modified with polymers with a high conductivity as well as SAM-modified tips can be used for STM measurements at molecular resolution.

4. DISCRIMINATION OF FUNCTIONAL GROUPS BASED ON CONTRAST CHANGES DUE TO HYDROGEN BOND INTERACTIONS BETWEEN CHEMICALLY MODIFIED TIPS AND SAMPLES /10-12/

Many researchers reported that the contrasts of hydroxyl, carboxyl, and ether groups of alkands, alkanoic acids, and dialkylethers, respectively, adsorbed on HOPG are darker than those of alkyl chains in STM images observed with unmodified metal tips /34,35/. Figures 3a, 4a and 5a show typical STM images of 1-octadecanol ($C_{18}H_{37}OH$), 1-octadecanoic acid ($C_{17}H_{35}COOH$) and dihexadecylether ($C_{16}H_{33}OC_{16}H_{33}$) that adsorb on HOPG as observed with unmodified gold tips. These images show lamella structures

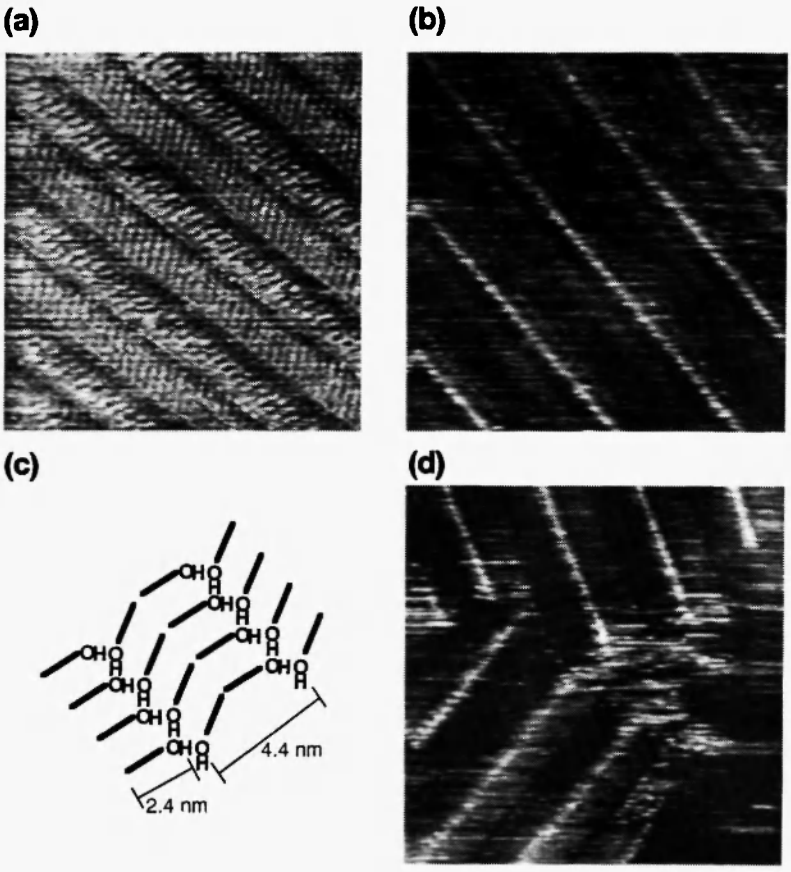

Fig. 3: (a) STM image of 1-octadecanol physisorbed from a 1-phenyloctane solution onto HOPG, as obtained with an unmodified gold tip. Image size 20 nm × 20 nm, total gray scale range 0.20 nm, sample bias voltage –1.00 V (sample negative), tunneling current 1.00 nA. (b) STM image of a 1-octadecanol monolayer on HOPG, as obtained with a **1**-modified gold tip. Image size 20 nm × 20 nm, total gray scale range 0.20 nm, sample bias voltage –1.00 V (sample negative), tunneling current 0.70 nA. (c) Schematic illustration of the molecular arrangement as observed for the monolayer of 1-octadecanol. Bars represent alkyl chains. (d) STM image of an interdomain structure in a 1-octadecanol monolayer on HOPG, as obtained with a **1**-modified gold tip. Image size 20 nm × 20 nm, total gray scale range 0.30 nm, sample bias voltage –0.80 V (sample negative), tunneling current 0.70 nA.

Fig. 4: (a) STM image of 1-octadecanoic acid ($C_{17}H_{35}COOH$) physisorbed from a 1-phenyloctane solution onto HOPG, as acquired with an unmodified gold tip. Image size 20 nm × 20 nm, total gray scale range 0.08 nm, sample bias voltage –0.70 V (sample negative), tunneling current 0.70 nA. (b) STM image of 1-octadecanoic acid physisorbed from a 1-phenyloctane solution onto HOPG, as obtained with a 1-modified gold tip. Image size 20 nm × 20 nm, total gray scale range 0.20 nm, Sample bias voltage +0.40 V (sample positive), tunneling current 0.70 nA. (c) Schematic illustration of the molecular arrangement as observed for the monolayer of 1-octadecanoic acid. Bars represent alkyl chains.

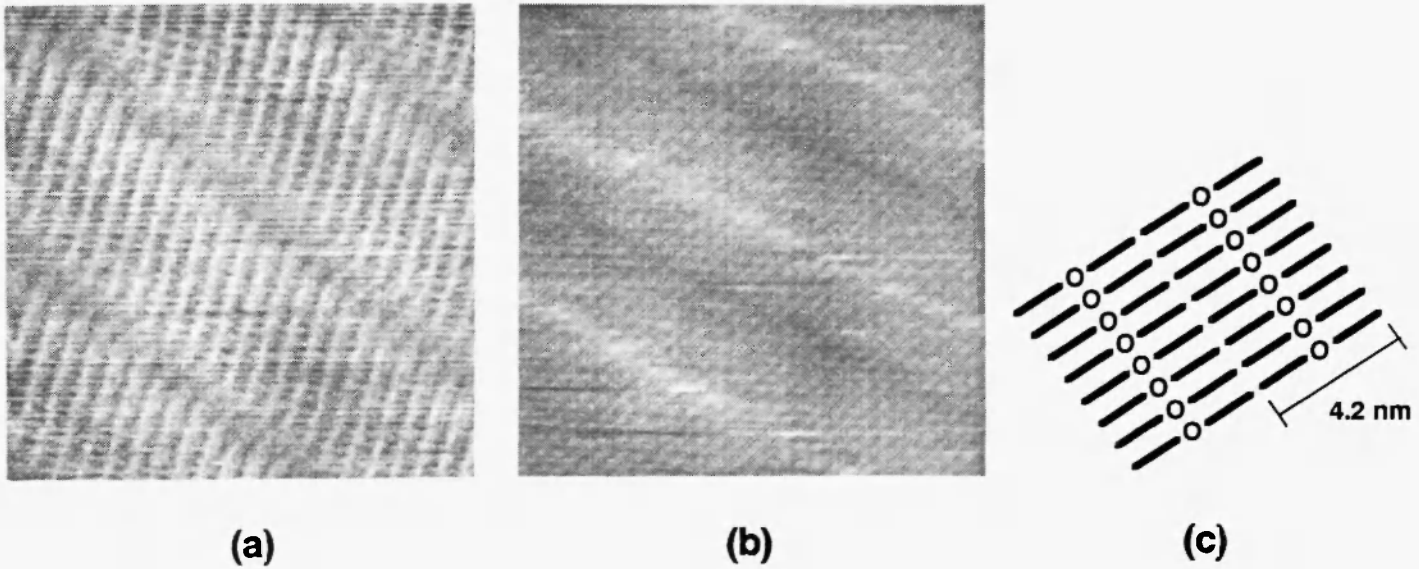

Fig. 5: (a) STM image of a dihexadecylether ($C_{16}H_{32}OC_{16}H_{33}$) monolayer physisorbed from 1-phenyloctane solution onto HOPG, observed with an unmodified gold tip. Image size 10 nm × 10 nm, total gray scale range 0.18 nm, sample-bias voltage –0.90 V (sample negative), tunneling current 0.70 nA. (b) STM image of a dihexadecylether monolayer observed with a 4-modified gold tip. Image size 10 nm × 10 nm, total gray scale range 0.45 nm, sample-bias voltage –0.90 V (sample negative), tunneling current 0.70 nA. (c) Schematic illustration of the molecular arrangement of dihexadecylether in the adsorbed monolayer. Bars represent alkyl chains.

consisting of parallel bands that correspond to individual molecules orienting parallel to the graphite surface, as supported by the coincidence between the length of the bands and the molecular length of these molecules with its alkyl chain in all-*trans* conformation (cf. schematic illustrations of the molecular arrangements were estimated as shown in Figures 3c, 4c and 5c, respectively). In these images, the hydroxyl group cannot exactly be assigned, because the terminal methyl groups were similarly observed as darker parts. The carboxyl groups and ether oxygens were observed as darker and a little brighter parts, respectively, than the terminal methyl groups. These functional groups can form hydrogen bond. Because of its relevance for biological charge transfer processes, electron transfer by tunneling through hydrogen bonds has recently attracted considerable attention /36/. We accordingly investigated the effect of hydrogen bond interactions on the STM contrasts of these functional groups by using tips modified with SAMs of thiols or thin films of polypyrroles.

As shown below, not all chemically modified tips prepared gave contrast changes originated from chemical interactions. Chemical modification of the tips was achieved by a conventional self-assembly method, which does not necessarily guarantee the presence of the modifying molecules at the tip apex. This probably explains the occasional failure in the observation of the contrast changes. STM images generally reflect the tunneling current through the overlap of the electronic wave functions between only small amount (usually one) of atom or molecule on the topmost of the tip. Most of spectroscopic and electrochemical methods, which give information on the average of surface, cannot be applied to check the chemical modification on the tip apex. We therefore evaluate the effect of the chemical modification of STM tips on the STM images from the fraction of the tips that gave contrast changes in all examined tips. In addition, even when contrast changes were initially observed with a certain chemically modified tip, the image was sometimes changed into the ones observed with unmodified tips after several-minutes' imaging under the identical condition. The loss of contrast changes may be due to removal of molecules from the STM tip apex during scanning, as also suggested in previous reports on tips with accidental adsorbates /14, 15, 23, 24, 26, 27/.

4.1. STM Tips Modified with Thiol SAMs /10,12/

For the above purpose, we first performed STM measurements by using tips modified with SAMs of thiols (**1**–**5**; Figure 2): 4-mercaptopyridine (**1**), 4-aminothiophenol (**2**), 4-hydroxythiophenol (**3**) or 4-mercaptobenzoic acid (**4**) and as a reference, thiophenol (**5**). The former four thiols have functional groups that can form hydrogen bonds as a hydrogen-bond acceptor (**1**) and as both hydrogen-bond acceptor and donor (**2**, **3**, **4**), whereas **5** has no such functional group. In the following, we summarize the contrast changes of the functional groups of alkanols, alkanoic acid and dialkylether on HOPG as observed with the SAM-modified tips.

a) Hydroxyl Groups /10/

Figure 3b shows STM images of 1-octadecanol monolayers that was formed at the solution–HOPG interface, as observed with a **1**-modified tip. Whereas hydroxyl end groups cannot be distinguished from the methyl groups in the images obtained with unmodified tips (Figure 3a), parallel bright lines separated by 4.4 ± 0.2 nm, which almost corresponds to twice the width of the lamella of 1-octadecanol (ca. 2.2 nm) and the separation of hydroxyl or methyl end groups in the monolayer (cf. Figure 3c), were observed in Figure 3b. Also at the domain regions of 1-octadecanol monolayers /34/, similar parallel bright bands were observed with **1**-modified tips (Figure 3d) /37/. In addition, **1**-modified tips gave similar contrast change for hydroxyl groups of 1-triacontanol ($C_{30}H_{61}OH$) monolayers (data not shown) /37/.

The contrast changes as shown in Figures 3b and d (contrast enhancements) were often observed with tips modified with SAMs having functional groups that can form hydrogen bonds. For example, the contrast change in 1-octadecanol monolayer was observed with tips modified with **1** (7 of 36 tips with which molecular images were observed; 19%) or **2** (8 of 26 tips; 31%) whereas not observed with unmodified tips (0 of 91 tips) and tips modified with **5** (0 of 27 tips). Tip modification with **3** gave lower frequency (3 of 31 tips; 10%). Also for 1-triacontanol monolayers, the contrast change in hydroxyl groups was observed with tips modified with **1** (4 of 30 tips; 13 %) in contrast to unmodified tips (0 of 71 tips). The contrast enhancements for 1-alkanol monolayers were more frequently observed with tips modified with organic mercaptans that have functional groups with stronger hydrogen-bond basicity: the order of the hydrogen-bond basicity is pyridine > aniline >

phenol. This suggests that hydrogen bond interactions between the functional groups on tip and sample involve the contrast enhancements for hydroxyl groups of 1-alkanol as shown in Figures 3b and 3d.

b) Carboxyl Groups /10/

Figure 4b shows STM images of 1-octadecanoic acid monolayers as acquired with a **1**-modified tip. Whereas the carboxyl end groups positioning at the lamella borders appeared as dark spots with unmodified tips (Figure 4a), each lamella has two borders that appear much brighter than the alkyl chains in Figure 4b. The proportion of tips that gave the images as shown in Figure 4b was higher for **1**-modified tips (6 of 36 tips; 17%) than for unmodified tips (3 of 90 tips; 3%), and additionally, the extent of the contrast enhancements as shown in Figure 4b was usually larger for **1**-modified tips than with unmodified tips (10). Images similar to that in Figure 4b were also observed with tips modified with **3** (6 of 28 tips; 21%), but were rarely observed with tips modified with **2** (1 of 23 tips; 4%) or **5** (0 of 26 tips). These results suggest that the contrast enhancements of carboxyl groups in 1-octadecanoic acid monolayer are also due to hydrogen bond interactions between the functional groups on tip and sample. However, in contrast to the alkanol monolayers, the order of the observation frequency of the enhanced images among tips modified with different mercaptans cannot be explained on the basis of the hydrogen-bond basicity (vide supra). In Figure 4b, the width of the enhanced region is ca. 1 nm, which is wider than that of the dark region corresponding to the carboxyl groups in Figure 4a (ca. 0.7 nm). The reason for this large width may be related to the large strength of hydrogen bonds to the carboxyl group, resulting in electron tunneling across longer distances.

c) Ether Oxygens /12/

In the above examples, tips modified with SAMs having hydrogen bond-accepting functional groups gave the enhanced contrast at hydroxyl and carboxyl groups in monolayers of primarily substituted hydrocarbons. Similar contrast enhancements were also observed for ether oxygens, which behave as only hydrogen bond acceptors, with tips modified with **4**, which behave as hydrogen bond donors. Figure 5b shows an STM image of a dihexadecylether monolayer observed with a **4**-modified tip. In Figure 5b, bright lines separated by 4.1 ± 0.6 nm from each other were observed, and

this separation agrees within an error with the sum of the length of a single dihexadecylether molecule and the intermolecular distance of the two ether oxygen atoms of the neighboring lamellae, as it is apparent from the images obtained with unmodified tips (Figure 5a). With the **4**-modified tips, 8 of 50 observations (16%) exhibited STM images with bright lines, while unmodified tips as well as **5**-modified tips rarely exhibited such bright lines (1 of 49 and 45 tips, respectively; 2%). This suggests that the contrast enhancements for ether oxygens are attributed to the tip modification with **4**, and an enhancement of the tunneling current due to hydrogen bond interaction between dihexadecylether and **4** on the tip likely explains the bright lines revealing the position of the ether oxygens.

The above three examples indicate that STM tips modified with SAMs having hydrogen-bond acceptors as well as donors gave the specific contrast enhancement for hydroxyl and carboxyl groups as well as ether oxygens of molecules adsorbed onto graphite on the basis of hydrogen bond interactions. The above conclusion is also supported by the absence of the contrast enhancement for STM images of 1-chlorooctadecane ($C_{18}H_{37}Cl$) monolayers observed with **1**-modified tips /10/. The similarity of the contrast enhancements under fairly wide range of tunneling conditions for all combinations of samples and chemically modified tips may also support the conclusion /10,12/. Electron tunneling through hydrogen bonds, as recently observed for photoinduced electron transfer /36/, probably occurs when the electronic wave functions of the hydrogen bond donor and acceptor groups overlap, resulting in the facilitation of electron tunneling and the contrast enhancements.

4.2. STM Tips Modified with Polypyrroles /11/

As shown in the above, SAM-modified tips gave the contrast enhancements for hydroxyl, carboxyl and ether groups on the basis of hydrogen bond interactions. However, only a limited number of SAM-modified tips (30% at most) allowed the observation of such selective contrasts. Drawing once more an analogy to chemically modified electrodes, we wondered whether use of polymer-modified tips could improve the experimental reproducibility. Polymer films are often used as electrode coatings and, due to their chemical and electrochemical stability, can considerably improve the reproducibility of electrochemical experiments /1/. We chose conducting polypyrrole for modification of STM tips because of its

high stability and the feasibility of its reproducible preparation, and most importantly because it can form hydrogen bonds through its nitrogen moieties.

Figure 6a shows an STM image of 1-octadecanol monolayer observed with BF_4^--doped polypyrrole. In Figure 6a, parallel, bright lines separated by ca. 4.7 nm, which again corresponds to twice the width of the lamella of 1-octadecanol and the separation of the two OH groups of the neighboring lamella, were observed. The proportion of tips that gave the contrast enhancements to the examined tips that gave molecular images depended strongly on how polypyrrole-modified tips were washed after the electrochemical polymerization. The fraction of tips that gave the contrast changes was higher for tips washed at pH 7 (13 of 26 tips that gave molecular images; 50%) than for those washed at pH 5.5 (5 of 31 tips, 16%) and 6 (5 of 23 tips; 22%), and was very small for washing at pH 2 (1 of 25 tips; 4%). This result suggests that basic, deprotonated polypyrrole subunits involve the contrast enhancements as shown in Figure 6a, because it has been reported that the NH moiety of polypyrrole subunits gradually deprotonates with increasing the pH of the solution in which polypyrrole are immersed (Figure 6b). This trend correlates to that observed with SAM-modified tips: the probability of the observation of contrast enhancements for alkanol monolayers seemed to reflect the hydrogen-bond basicity of the functional groups in the tip-modifying molecules. Thus, it can be concluded that hydroxyl groups in the sample monolayer were shown as the bright areas observed with polypyrrole-modified tips due to hydrogen bond interactions between hydroxyl groups in the sample monolayer and deprotonated pyrrole subunits in the polymer. Contrast enhancements with BF_4^--doped polypyrrole were also observed for carboxyl groups in images of monolayers of 1-octadecanoic acid /11/.

STM images obtained with polypyrrole-modified tips have more noise than those obtained with SAM-modified tips, and as a result, the resolution of images observed with polypyrrole-modified tips (e.g. Figure 6a) was somewhat lower than that with SAM-modified tips (e.g., Figure 3b). A decrease in the conductivity of the film as well as the enlargement of tip radius probably explain these results. However, the proportion of tips that gave the contrast enhancements was higher for BF_4^--doped polypyrrole (50% at most) than for SAM-modified tips (up to 31%). This suggests that modification of tips with conducting polymers is also promising for functional group recognition with STM.

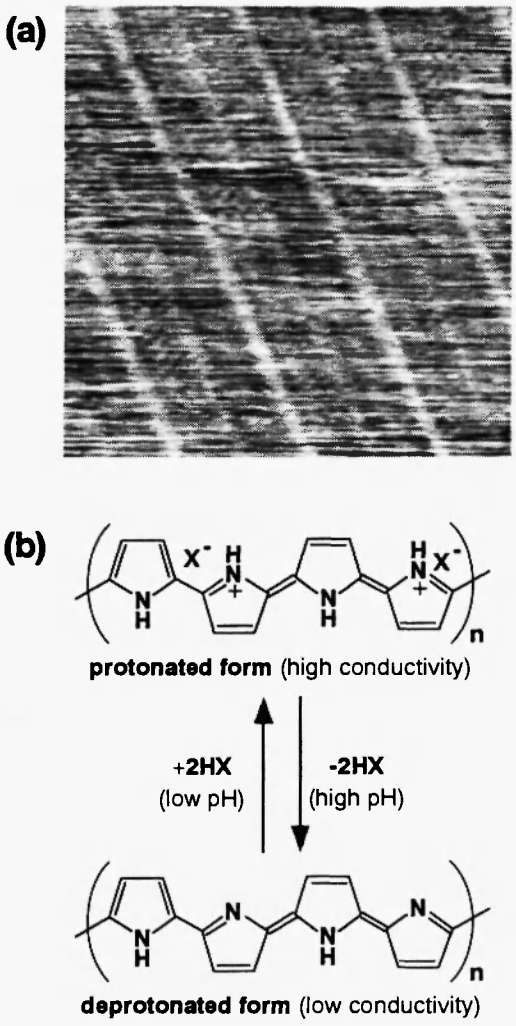

Fig. 6: (a) STM image of a 1-octadecanol monolayer physisorbed from 1-phenyloctane solution onto HOPG, measured with a gold tip modified with BF_4^--doped polypyrrole (film thickness ca. 0.8 μm) and washed in a 1 mM phosphate buffer containing 0.1 M $NaBF_4$ (pH 7). Image size 20 nm × 20 nm, total gray scale range 0.70 nm, sample bias voltage 1.00 V (sample positive), tunneling current 1.00 nA. The height of the bright lines of OH groups as compared to the rest of the lamella was ca. 0.07 nm. (b) Effect of pH on the protonation/deprotonation of polypyrroles.

5. DETERMINATION OF THE ORIENTATION OF ETHER OXYGENS WITH STM BY USING CHEMICALLY MODIFIED TIPS /12/

In the above chapter, we showed that STM imagings with chemically modified tips gave the selective contrast enhancements for hydroxyl and carboxyl groups as well as ether oxygens on the basis of hydrogen bond interactions between functional groups on tip and sample. It is well-known that the strength of hydrogen bonds depends on the relative orientation of the hydrogen bond-donors and hydrogen bond-acceptors because different orientations result in a varying extent of orbital overlap. It is therefore expected that the extent of the contrast enhancements also depends on the orientation of the functional groups. To demonstrate this, we compared the contrasts among ether oxygens in molecular STM images of diethers $CH_3(CH_2)_{15}O(CH_2)_nO(CH_2)_{15}CH_3$ (n = 9–12, hereafter abbreviated to $C_{16}OC_nOC_{16}$) observed with **4**-modified tips, which gave the contrast enhancement for ether oxygens (see section **4.1c**). These diethers can be classified into two groups: diethers with even-membered (n = 10 and 12) and odd-membered spacers (n = 11 and 13). In all-*trans* conformation, the non-bonding oxygen orbitals of the former diethers point in opposite directions, whereas those of the latter point in the same direction.

Figures 7a and 8a show STM images of $C_{16}OC_9OC_{16}$ and $C_{16}OC_{12}OC_{16}$ monolayers respectively, observed with unmodified gold tips. In both images, ether oxygens were observed darker than hydrocarbon backbones with unmodified tips for both monolayers as similarly with dihexadecylether (Figure 5a). In contrast, **4**-modified tips gave two bright lines that correspond to the distribution of the ether oxygens for $C_{16}OC_9OC_{16}$ and $C_{16}OC_{12}OC_{16}$ monolayers (Figures 7b and 8b, respectively) /12/. The contrast changes for the diether monolayers are again probably due to hydrogen bond interactions between the tips and samples. The frequencies of the contrast enhancements in both monolayers with the **4**-modified tips were comparable with those in dihexadecylether as discussed above. Interestingly, one bright line is significantly higher than the other one for the $C_{16}OC_{12}OC_{16}$ monolayer (Figure 8c), whereas the heights of the two bright lines are similar for the $C_{16}OC_9OC_{16}$ monolayer (Figure 7c). Similar trends in STM images observed with **4**-modified tips were also obtained in the images of $C_{16}OC_{10}OC_{16}$ and $C_{16}OC_{11}OC_{16}$ monolayers (Figures 8c and 7c), respectively, indicating that the extent of the contrast enhancement is similar for two ether oxygens of the

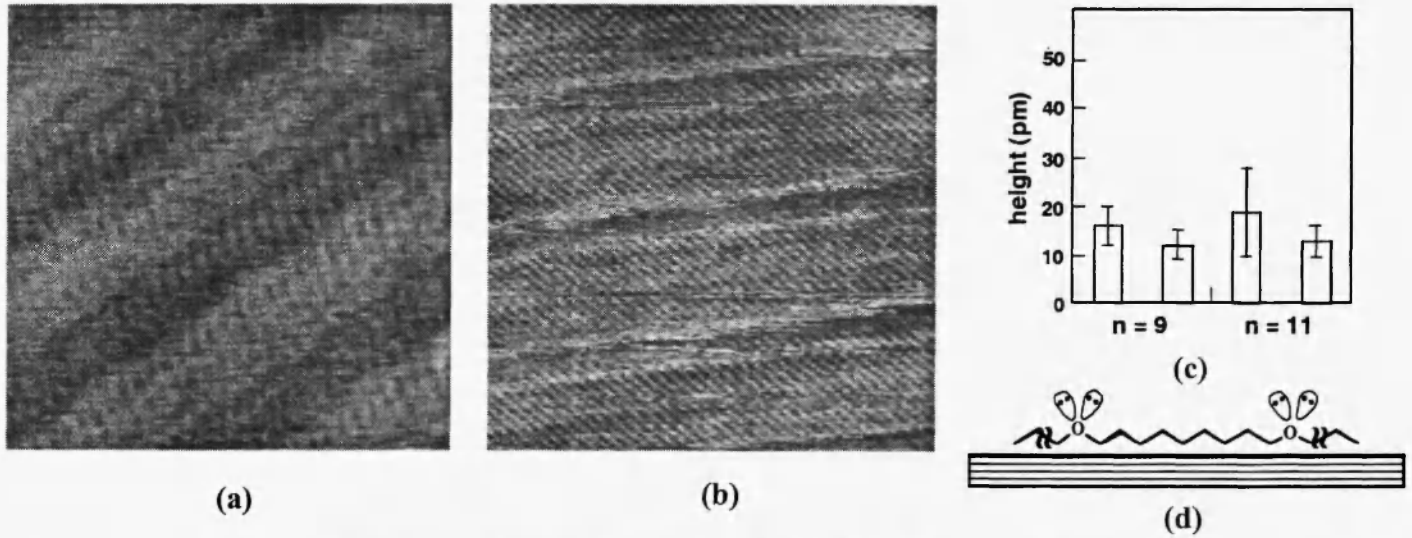

Fig. 7: (a) STM image of a 1,9-bis(hexadecyloxy)nonane ($C_{16}OC_9OC_{16}$) monolayer physisorbed from a 1,2,4-trichlorobenzene solution onto HOPG, measured with an unmodified gold tip. Image size 15 nm × 15 nm, total gray scale range 0.15 nm, sample-bias voltage –0.90 V (sample negative), tunneling current 0.70 nA. (b) STM image of a $C_{16}OC_9OC_{16}$ observed with a **4**-modified gold tip. Image size 15 nm × 15 nm, total gray scale 0.18 nm, sample-bias voltage –0.90 V (sample negative), tunneling current 0.70 nA. (c) Bar graph showing the brightness (height) of the two bright lines pertaining to the same lamella in STM images of diethers with odd-membered spacers ($C_{16}OC_nOC_{16}$; n = 9, 11), as observed with **4**-modified tips. The heights are relative with respect to the height of the alkyl chains. (d) Schematic illustration of diether with odd-membered spacer adsorbed onto basal plane of HOPG.

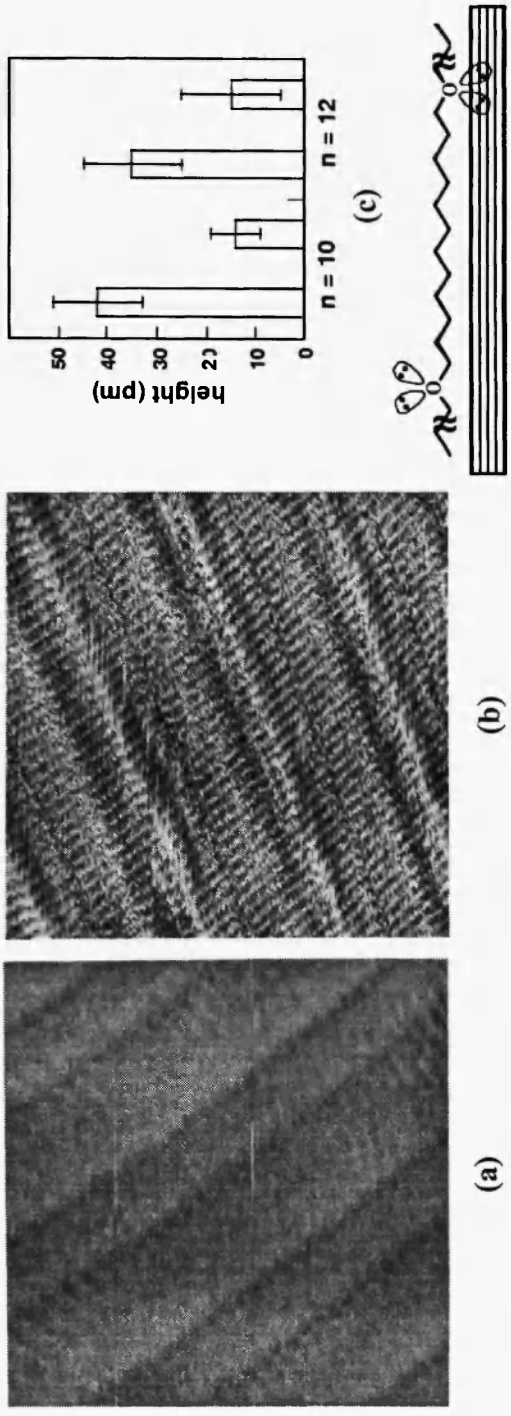

Fig. 8: STM images of the monolayer of 1,12-bis(hexadecyloxy)dodecane ($C_{16}OC_{12}OC_{16}$) physisorbed from a 1,2,4-trichlorobenzene solution onto HOPG, measured with (a) an unmodified gold tip and (b) a 4-modified tip. Image size 15 nm × 15 nm, sample-bias voltage –0.90 V (sample negative), tunneling current 0.7 nA. Total gray scale range (a) 0.15 nm, (b) 0.3 nm. (c) Bar graph showing the brightness (height) of the two bright lines pertaining to the same lamella in STM images of diethers with even-membered spacers ($C_{16}OC_nOC_{16}$; n = 10, 12), as observed with 4-modified tips. The heights are relative with respect to the height of the alkyl chains. (d) Schematic illustration of diether with even-membered spacer adsorbed onto basal plane of HOPG.

diethers with odd-membered spacers whereas that is quite different for those with even-membered spacers.

This difference indicates that the diethers with even- and odd-membered spacers are adsorbed with the carbon skeletal planes perpendicular to the HOPG surface, and accordingly can be explained on the basis of the orientation of these ether oxygens. In the case of the diethers with even-membered spacers in perpendicular orientation, the orbitals of one oxygen point down to the HOPG surface, and the lone-pair orbitals of the second oxygen point up towards the STM tip (Figure 8d). Because the orientation in which the donor and acceptor directly face each other is most favorable for hydrogen bond formation, the oxygen atom with the lone-pair electrons pointing upwards can form a stronger hydrogen bond with **4** on the tip than the oxygen with the lone-pair orbitals pointing downwards. This difference in the strength of the hydrogen bond causes the difference in the brightness for the two oxygens. Enhanced contrasts were also observed to a lesser extent for the ether oxygens pointing downwards to the HOPG surface, suggesting a hydrogen bond interaction between these oxygens and **4** on the tip. This weak hydrogen bond interaction may be explained by the fact that the lone-pair electron orbitals of these ether oxygens are oriented at an angle of approximately 55¡ relative to the surface normal when the carbon skeletal planes of the diethers are normal to the surface. This conformation is quite unfavorable but still allows some interaction with the modified tip. In the case of diethers with odd-membered spacers, the two ether oxygens point in the same direction and allow the hydrogen bond interaction with the same strength with **4** on the tip (Figure 7d). As a result, no difference in the brightness of the bright lines was observed.

The above results strongly supports the significance of hydrogen bond interactions between tips and samples for the contrast enhancements, and additionally demonstrate that STM imagings with chemically modified tips allow not only the discrimination of functional groups but also the determination of the orientation of the functional groups.

6. DISCRIMINATION OF PORPHYRIN CENTERS BASED ON METAL-COORDINATION AND HYDROGEN BOND INTERACTIONS /13/

In the above chapters, we showed that hydrogen bond interactions between chemically modified tips and sample monolayers induce the contrast

enhancements for the functional groups that can form hydrogen bonds in STM images. The contrast changes can be explained on the basis of the enhancement of electron tunneling through the overlap of molecular orbitals due to hydrogen bond interactions between tip-modifying molecules and sample functional groups. The overlap of molecular orbital occurs on the other chemical interactions such as metal-coordination interaction. We therefore extend the idea of STM measurements with chemically modified tips toward metal-coordination interactions similarly to hydrogen bond interactions.

Porphyrins having two long alkyl chains at trans positions (**8**–**10**; Figure 2) were used as samples, because the porphyrins were expected to adsorb strongly to graphite surface through their long alkyl chains and as a result, form their monolayers. Before our study, several researchers reported STM images of phthalocyanines and porphyrins with unmodified metal tips. With regard to the contrast of central metals in these complexes, Lu *et al.* reported that cobalt atom in cobalt phthalocyanine on Au(111) gave the highest point in the STM image of the molecule whereas the copper atom in copper phthalocyanine on Au(111) appeared as a depression /38,39/. The former contrast was explained by a large contribution of the cobalt *d*-orbitals near the Fermi energy. Also in aqueous solutions, molecular images of iron (III) protoporphyrin (IX), zinc (II) protoporphyrin (IX) and metal-free protoporphyrin (IX) were observed, and their observed internal structures were shown to be different (40). Here, we used metal-free porphyrin (Por-H_2 (**8**)) as well as zinc and nickel porphyrins (Por-Zn (**9**) and Por-Ni (**10**), respectively) as samples, whose central parts were similarly observed as depressions with unmodified metal tips (vide infra). Images of these porphyrins were observed with tips modified with 4-mercaptopyridine (**1**), whose pyridyl group is expected to form not only hydrogen bond but also metal-coordination interactions to central parts of the porphyrins.

Figure 9a shows a typical STM image of a mixed monolayer of Por-Zn and Por-Ni (molar ratio in a 1,2-dichlorobenzene solution; Por-Zn : Por-Ni = 1.00 : 0.33) observed with an unmodified tip. The diameter of the ring (1.1 ± 0.2 nm) is consistent with that of the porphyrin ring as estimated from a CPK model, indicating that the porphyrins adsorb horizontally on the graphite surface. The centers of Por-Zn and Por-Ni in Figure 9a appear as dark depressions, and these porphyrins cannot be distinguished from each other. In contrast, chemically modified tips gave very different images. Figure 9b shows STM image of a mixed monolayer of Por-Zn and Por-Ni

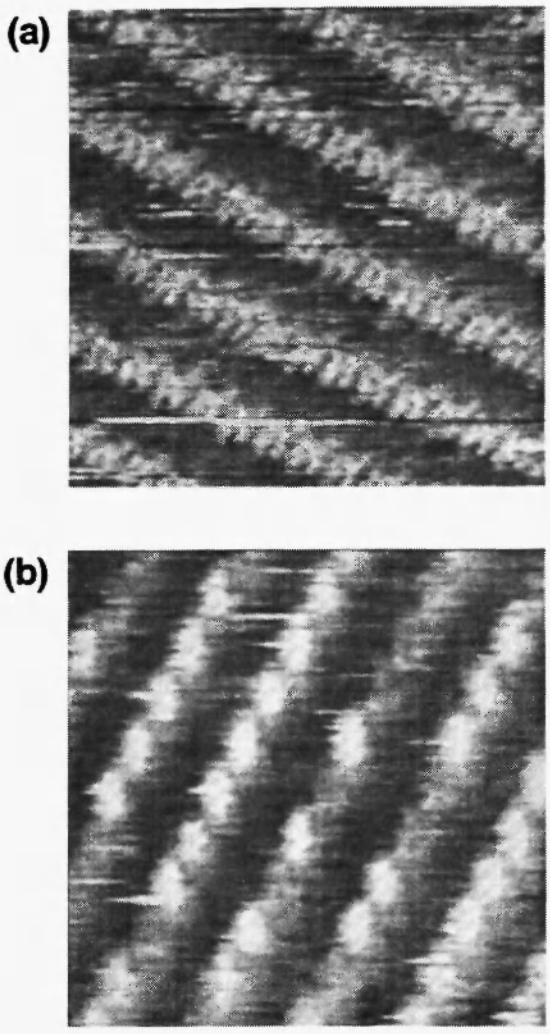

Fig. 9: (a) STM image of mixed monolayer of Por-Zn and Por-Ni (molar ratio in the sample solution; Por-Zn : Por-Ni = 1.00 : 0.33) physisorbed from a 1,2-dichlorobenzene solution onto HOPG, obtained with an unmodified Pt/Ir tip. Image size 15 nm × 15 nm, total gray scale range 0.5 nm, sample-bias voltage −1.02 V (sample negative), tunneling current 0.46 nA. (b) STM image of mixed monolayer of Por-Zn and Por-Ni (molar ratio in the sample solution; Por-Zn : Por-Ni = 1.00 : 0.33) obtained with a **1**-modified tip. Image size 15 nm × 15 nm, total gray scale range 0.3 nm, sample-bias voltage −1.15 V (sample negative), tunneling current 0.32 nA.

(Por-Zn : Por-Ni = 1.00 : 0.33) observed with **1**-modified gold tips. In Figure 9b, the size of the porphyrin rings is similar to that in Figure 9a, but the central parts of the porphyrin rings appeared as bright spots. The presence and absence of the bright contrast with **1**-modified and unmodified tips, respectively, suggest that the contrast change is due to metal-coordination interactions between molecules on tips and the metalloporphyrins.

Interestingly, two types of the bright spots were observed: "very bright" and "moderately bright" spots. The ratio of the number of "very bright" and "moderately bright" spots was approximately 1.00 : 0.29 for Figure 9b, which is quite close to the molar ratio of Por-Zn and Por-Ni in the sample solution. The ratio of "very bright spots" in STM images observed with **1**-modified tips increased with increasing the molar ratio of Por-Zn in sample solutions. In addition, the height of the porphyrin centers relative to its ring height (h_{center}/h_{ring}; mean value ± standard deviation), which are defined as the ratio of the vertical distances between the porphyrin center and the porphyrin ring against the alkyl chains, were 2.3 ± 0.4 for the "very bright spots" and 1.5 ± 0.2 for the "moderately bright spots", and these values almost corresponded to those of STM images of pure Por-Zn (2.0 ± 0.2) and Por-Ni (1.5 ± 0.2) monolayers, respectively, observed in their pure monolayers with **1**-modified tips /13/. The h_{center}/h_{ring} values of Por-Zn and Por-Ni obtained with unmodified tips were 0.5 ± 0.1 and 0.4 ± 0.1, respectively, suggesting that the porphyrin centers were indeed observed as depressions. These indicate that the "very bright" and "moderately bright" spots are Por-Zn and Por-Ni, respectively.

It is well known that axial coordination of neutral ligands such as pyridine to metalloporphyrins is much stronger for zinc porphyrin than for nickel porphyrin /41/. Therefore, the difference of contrasts of the porphyrin centers probably reflects the magnitude of the metal-coordination interaction between the pyridyl group of **1** on the tips and the central metals of the porphyrins. Large overlap of molecular orbitals seems to allow not only the strong coordination interaction but also the large enhancement of electron tunneling between tip and sample.

Similar results were also observed for mixed monolayers of Por-Zn and Por-H_2 with **1**-modified tips. Figure 10a shows a typical STM image of the mixed monolayer (molar ratio in a 1,2-dichlorobenzene solution; Por-Zn : Por-H_2 = 1.00 : 2.00) observed with an unmodified tip. Similar to the STM image of mixed monolayer of Por-Zn and Por-Ni (Figure 9a), the centers of Por-Zn and Por-H_2 in Figure 10a appear as dark depression as suggested by

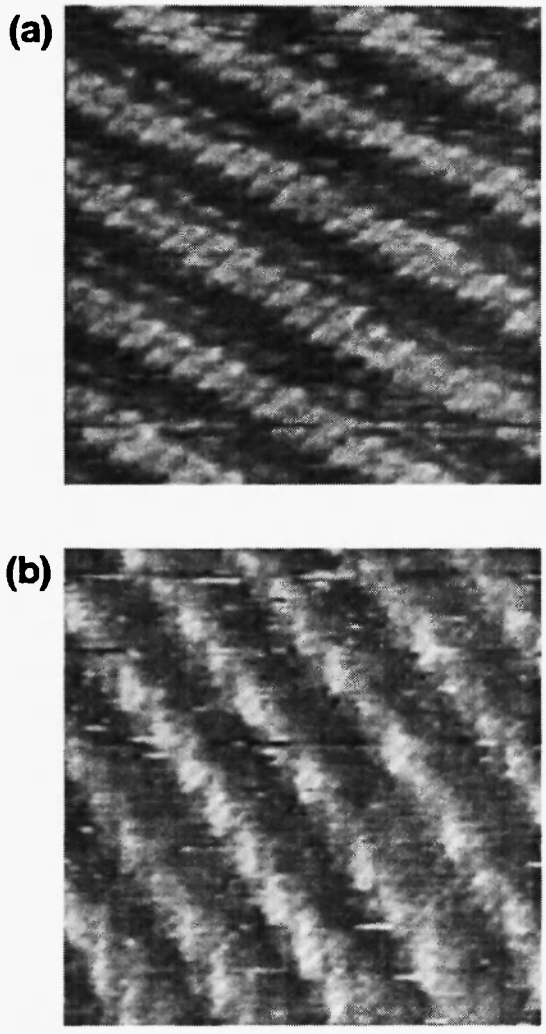

Fig. 10: (a) STM image of mixed monolayer of Por-Zn and Por-H_2 (molar ratio in the sample solution; Por-Zn : Por-H_2 = 1.00 : 2.00) physisorbed from a 1,2-dichlorobenzene solution onto HOPG, obtained with an unmodified Pt/Ir tip. Image size 15 nm × 15 nm, total gray scale range 0.5 nm, sample-bias voltage –0.70 V (sample negative), tunneling current 0.38 nA. (b) STM image of mixed monolayer of Por-Zn and Por-H_2 (molar ratio in the sample solution; Por-Zn : Por-H_2 = 1.00 : 0.50) obtained with a **1**-modified tip. Image size 15 nm × 15 nm, total gray scale range 1.2 nm, sample-bias voltage –0.81 V (sample negative), tunneling current 0.33 nA.

the h_{center}/h_{ring} values of Por-Zn and Por-H_2 in their pure monolayers obtained with unmodified tips (0.5 ± 0.1 and 0.4 ± 0.1, respectively), and these porphyrins cannot be distinguished from each other. In contrast, Figure 10b shows STM image of mixed monolayer of Por-Zn and Por-H_2 (Por-Zn : Por-H_2 = 1.00 : 0.50) observed with **1**-modified gold tips. The central parts of the porphyrins appeared as two types of bright spots, i.e., "very bright" and "moderately bright" spots, whereas the size and shape of the porphyrin rings are similar to those in Figure 10a. The h_{center}/h_{ring} values were 2.5 ± 0.6 for the "very bright spots" and 1.4 ± 0.2 for the "moderately bright spots", and these values almost corresponded to those of STM images of pure Por-Zn (2.0 ± 0.2) and Por-H_2 (1.5 ± 0.2) monolayers, respectively, observed with **1**-modified tips /13/. These indicate that the "very bright" and "moderately bright" spots are Por-Zn and Por-H_2, respectively. Indeed, the ratio of the number of "very bright" and "moderately bright" spots was 1.00 : 0.47 for Figure 10b, which is quite close to the molar ratio of Por-Zn and Por-H_2 in the sample solution. The contrast change for Por-H_2 was probably induced by the hydrogen bond interactions between the pyridyl group of **1** on the STM tip and the two nitrogen-bound hydrogens of Por-H_2. Figure 10b shows that the metal-coordination interaction between the central zinc of Por-Zn and **1**-modified tip increases the tunneling current more than the hydrogen bonds between the N-H hydrogen of Por-H_2 and **1**-modified tip, and that each porphyrin can be possibly identified on the basis of their h_{center}/h_{ring}.

As shown above, contrast enhancements at the porphyrin centers were induced not only through hydrogen bond interactions but also through metal-coordination interactions by chemically modified tips. The contrast changes in STM images obtained with **1**-modified tips allow to discriminate Por-Zn from Por-H_2 and Por-Ni.

7. CONCLUSIONS

In this review, we described our studies on STM with chemically modified tips. When chemically modified tips were used for STM measurements, contrast enhancements at specific regions in STM images occurred on the basis of hydrogen bond and metal-coordination interactions, and as a result, allowed to detect not only the distribution of specific chemical species and functional groups but also the orientation of functional groups. The contrast enhancements seemed to reflect the increase in a

tunneling current due to the overlap of electronic wave functions induced by the chemical interactions between tip and sample. Although we have not understood the imaging mechanism of the contrast enhancements in detail, this principle for STM imagings with chemically modified tips may result in different selectivity as compared with chemical force microscopy, which discriminates surface functional groups only through interaction forces between tip and sample /8,9/. In addition, STM imagings with chemically modified tips usually give images with higher resolution (molecular resolution) as compared with chemical force microscopy. More selective discrimination of individual chemical species and functional groups may be possible by a rational use of multitopic interactions, as they are necessary for recognition of more complex chemical units such as oligonucleotides.

ACKNOWLEDGMENTS

This work was partially supported by Grants for Scientific Research from the Ministry of Education, Science and Culture, Japan, by the Nissan Science Foundation, and by Ogasawara Foundation.

REFERENCES

1. R.W. Murray, A. G. Ewing and R. A. Durst, *Anal. Chem.*, **59**, 379A (1987).
2. E. Grushka, Ed., *Bonded Stationary Phases in Chromatography*, Ann Arbor Science Publication, Ann Arbor, 1974.
3. L.R. Snyder and J.J. Kirkland, *Introduction to Modern Liquid Chromatography*, John Wiley & Sons, New York, 1979.
4. A. Ulman, *An Introduction to Ultrathin Organic Films: from Langmuir–Blodgett to Self-Assembly*, Academic Press, London, 1991.
5. R. Wiesendanger, *Scanning Probe Microscopy and Spectroscopy: Methods and Applications*, University Press, New York, 1994.
6. R. Wiesendanger and H.-J. Güntherodt, Eds., *Scanning Tunneling Microscopy I : General Principles and Applications to Clean and Adsorbate-Covered Surfaces*, Springer, Berlin, 1994.

7. R. Wiesendanger and H.-J. Güntherodt, Eds., *Scanning Tunneling Microscopy II : Further Applications and Related Scanning Techniques*, Springer, Berlin, 1995.
8. R. McKendry, M.-E. Theoclitou, C. Abell and T. Rayment, *Jpn. J. Appl. Phys.*, **38**, 3901 (1999).
9. H. Takano, J.R. Kenseth, S.-S. Wong, J. C. O'Brien and M.D. Porter, *Chem. Rev.*, **99**, 2845 (1999).
10. T. Ito, P. Bühlmann and Y. Umezawa, *Anal. Chem.*, **70**, 255 (1998).
11. T. Ito, P. Bühlmann and Y. Umezawa, *Anal. Chem.*, **71**, 1699 (1999).
12. T. Nishino, P. Bühlmann, T. Ito and Y. Umezawa, submitted.
13. T. Ohshiro, T. Ito, P. Bühlmann and Y. Umezawa, submitted.
14. J. Resh, D. Sarkar, J. Kulik, J. Brueck, A. Ignatiev and N. J. Halas, *Surf. Sci.*, **316**, L1061 (1994).
15. K.F. Kelly, D. Sarkar, S. Prato, J. S. Resh, G.D. Hale and N.J. Halas, *J. Vac. Sci. Technol. B*, **14**, 593 (1996).
16. K.F. Kelly, D. Sarkar, S.J. Oldenburg, G.D. Hale and N.J. Halas, *Synth. Metals*, **86**, 2407 (1997).
17. K.F. Kelly, D. Sarkar, G.D. Hale, S. J. Oldenburg and N.J. Halas, *Science*, **273**, 1371 (1996).
18. K.F. Kelly and N.J. Halas, *Surf. Sci.*, **416**, L1085 (1998).
19. H. Dai, J.H. Hafner, A.G. Rinzler, D.T. Colbert and R.E. Smalley, *Nature*, **384**, 147 (1996).
20. P. Sautet, J.C. Dunphy, D.F. Ogletree, C. Joachim and M. Salmeron, *Surf. Sci.*, **315**, 127 (1994).
21. B.J. McIntyre, P. Sautet, J.C. Dunphy, M. Salmeron and G.A. Somorjai, *J. Vac. Sci. Technol. B*, **12**, 1751 (1994).
22. L. Bartels, G. Meyer and K.-H. Rieder, *Surf. Sci.*, **432**, L621 (1999).
23. H. Xu and K. Y. S. Ng, *Surf. Sci.*, **355**, L350 (1996).
24. M. Schmid, H. Stadler and P. Varga, *Phys. Rev. Lett.*, **70**, 1441 (1993).
25. A. Biedermann, M. Schmid and P. Varga, *Fresenius J. Anal. Chem.*, **349**, 201 (1994).
26. L. Ruan, F. Besenbacher, I. Stensgaard and E. Laegsgaard, *Phys. Rev. Lett.*, **70**, 4079 (1993).
27. S. Rousset, S. Gauthier, O. Siboulet, W. Sacks, M. Belin and J. Klein, *Phys. Rev. Lett.*, **63**, 1265 (1989).
28. L. Bartels, G. Meyer and K.-H. Rieder, *Appl. Phys. Lett.*, **71**, 213 (1997).

29. J.G. Kushmerick, K.F. Kelly, H.-P. Rust, N.J. Halas and P.S. Weiss, *J. Phys. Chem. B*, **103**, 1619 (1999).
30. P. Sautet, *Surf. Sci.*, **374**, 406 (1997).
31. P. Sautet, *Chem. Rev.*, **97**, 1097 (1997).
32. G.A. Tsirlina, O.A. Petrii and S.Y. Vassiliev, *Electrochim. Acta*, **41**, 1887 (1996).
33. A. Diaz and J. Bargon, in: *Electrochemical Synthesis of Conducting Polymers*, ed. by T.A. Skotheim, Marcel Dekker, New York, 1986, p. 81.
34. D.M. Cyr, B. Venkataraman and G.W. Flynn, *Chem. Mater.*, **8**, 1600 (1996).
35. L.C. Giancarlo and G.W. Flynn, *Acc. Chem. Res.*, **33**, 491 (2000).
36. P.J.F. de Rege, S.A. Williams and M.J. Therien, *Science*, **269**, 1409 (1995).
37. T. Ito, PhD Thesis, The University of Tokyo, Tokyo, 1998.
38. X. Lu, K.W. Hipps, X.D. Wang and U. Mazur, *J. Am. Chem. Soc.*, **118**, 7197 (1996).
39. K.W. Hipps, X. Lu, X.D. Wang and U. Mazur, *J. Phys. Chem.*, **100**, 11207 (1996).
40. N.J. Tao, G. Cardenas, F. Cunha and Z. Shi, *Langmuir*, **11**, 4445 (1995).
41. J.W. Buchler, in: *Porphyrins and Metalloporphyrins*, ed. by K.M. Smith, Elsevier, Amsterdam, 1975.